The Journal of Engine Research

Winter 2024, Vol. 70, No. 4, pp. 1-13

Journal Homepage: www.engineresearch.ir

Original Research

CFD simulation of wall film during fuel injection and combustion in a three-cylinder turbocharged gasoline direct injection engine

Arash Mohammadi[1*], Nima Ajami[2], AmirHossein Parivar[2], Peyman sharghi[2]

[1] Mechanical Engineering Department, Shahid Rajaee Teacher Training University, Tehran, Iran
[2] Irankhodro Powertrain Company (IPCo), Tehran, Iran

ARTICLE INFO

Keywords:
GDI
Injector
Mixture Preparation
Spray Modeling

ABSTRACT

In this research, a 3D-CFD model was created to investigate the behavior of spray and combustion in a three-cylinder GDI engine using a six-hole nozzle injector. To validate the model, in-cylinder data pressure was conducted at Iran Khodro Power Train Company (IPCO) under wide-open throttle and 5500 rpm conditions. The obtained data were incorporated into the CFD model to simulate the spray evolution and combustion process inside the cylinder during fuel injection. Droplet temperature and lambda distribution from 30 deg to 279 deg after injection Were displayed. Temperature distribution during 2 to 40 deg ATDC was illustrated in the paper. Finally, evaporated fuel and wall film of the cylinder head, liner, and piston. Intake and exhaust valves and equivalence ratio in the combustion chamber have been studied.

* Corresponding author
E-mail address: amohammadi@sru.ac.ir (A. Mohammadi)

Received 27 April 2024; Accepted 19 May 2024
E-ISSN: 2345-4121/ISSN: 1735-5214

Cite this article: Mohammadi A, Ajami N, Parivar AH, Sharghi P. CFD simulation of wall film during fuel injection and combustion in a three-cylinder turbocharged gasoline direct injection engine. The Journal of Engine Research. 2024 Feb 20;70(4):1-13. doi: 10.22034/ER.2024.2025014.1034

1- Introduction

Internal Combustion Engines (ICEs) are commonly utilized in power generation, ships, locomotives, aerial transportation, and various mobility applications. Most of the ICEs rely on fossil fuels, particularly diesel and gasoline engines. However, these engines release harmful gases such as nitrogen oxides (NOx), carbon monoxide (CO), and particulate matter (PM), which pose risks to human health. Strict regulations such as European Limits and the Environmental Protection Agency (EPA) require automotive manufacturers to enhance ICEs to meet acceptable emission levels and improve engine efficiency. The Gasoline Direct Injection (GDI) strategy allows Spark Ignition (SI) engines to achieve better fuel economy and reduced emissions. Goliath and Gutbrod first employed the GDI strategy in the automotive industry in 1952 to power a two-stroke gasoline engine. Meanwhile, Mercedes Benz utilized it for the 300SL model with a four-stroke engine. In 1996, Mitsubishi introduced the first modern GDI engine for the Japanese and European markets, which was designed to operate with stratified and homogenous charge strategies at medium- and high-load operating conditions. Other manufacturers subsequently adopted Mitsubishi's strategy and developed their own engines.

The primary advantage of the GDI strategy is that it allows mixture preparation to occur in the combustion chamber, overcoming the limitations of Port Fuel Injection (PFI) and benefiting from the direct injection cooling effect to achieve higher compression ratios. The thermo-fluid dynamics in the combustion chamber significantly influence mixture formation in GDI engines. Factors such as piston shape, injector position, intake ports, and valve seat geometry heavily impact tumble and swirl ratios. Additionally, the injector nozzle number, injection pressure, sequential injection timing, and injection direction also affected the mixture formation [1-7]. Banerjee et al. [8] investigated the effects of mixture preparation in a GDI engine, they studied the impact of ambient pressure, ambient temperature, and fuel temperature on spray atomization for an injector with a single nozzle. They found that changes in ambient pressure and temperature significantly influenced spray penetration. Piston shape also had notable effects on charge stratification due to the reverse tumble at the end of the compression ratio. Addepalli et al. [9] conducted a computational fluid dynamics (CFD) analysis on the effect of mixture preparation on emissions and engine performance in a GDI engine. They reported that the early fuel injection did not have any significant impact on mixture preparation. The direction of the injector was also studied, and the results showed that deviations from the base direction affected mixture preparation. Additionally, they found that the mixture stratification in a wall-guided GDI engine was more sensitive to the engine speed and inlet air pressure, but less affected by the compression ratio. When the engine speed increased from 2000 to 3000 rpm, the percentage of evaporated fuel also increased. Zhaung et al. [10] discussed the influence of the direct injection of water into the cylinder on the combustion of gasoline direct injection engines through numerical simulation Zhaung et al. [11] explored the effects of six different cases of port water injection on the combustion, knock suppression and emissions of a supercharged GDI engine through numerical simulation. The six different intake port water injection cases including three vertical distances from the cylinder center to the water injector and two different injection directions, were investigated. Xiang et al. [12] investigated both the macroscopic and microscopic characteristics of impingement spray from a GDI injector fueled with gasoline and ethanol performed under injection pressure up to 50 MPa, providing new findings to promote a more homogeneous air-fuel mixture and reduce PM emissions. Heechang et al. [13] studied the spray chamber and injector conditions including (1) cold, subcooled standard temperature and pressure (2) practical gasoline fuels with full-range distillation, (3) flash-boiling with fuel temperature and vacuum gas pressure, and (4) high gas pressure and temperature typical of injection during compression.

Lili et al. [14] investigated GDI fuel spray characteristics, and spray impingement on

cylinder-wall oil film was carried out in a constant volume chamber. Quito et al. [15] studied a series of comparative experiments conducted on a GDI turbocharged engine to investigate the effects of the asynchronous intake valve Miller cycle on the performance, combustion, and emissions characteristics. Their results show that using the asynchronous valve closing in the test engine can not only realize the Miller cycle but also flexibly control the load, effectively reduce pump loss, and improve fuel economy compared to the late intake valve closing. Modapour et al. [16] adopted a combined experimental and numerical approach to examine the influence of wall temperature as well as gas temperature and pressure on spray evolution. For fuel injection conditions, split proportion and wall stand-off distance are not varied. The single injection case was also studied for comparison. The experiments were conducted under atmospheric conditions but for different wall temperatures, and the fuel spray was visualized using a high-speed shadowgraph technique. Berni et al. [17] applied 3D Computational Fluid Dynamics with several models to simulate the secondary break-up process, among which the Reitz-Diwakar and the Kelvin-Helmholtz Rayleigh-Taylor. To improve the predictive capabilities and reduce the need for case-by-case tuning, they applied an alternative secondary break-up model proposed in the present paper. It was based on the Reitz-Diwakar one but, compared to the latter, a zonalization of the break-up regimes.

In this study, a 3D-CFD model was developed to predict the spray evolution, mixture preparation, and combustion in a three-cylinder GDI 1.3-liter engine operated at 5500 rpm and wide-open throttle conditions. A side-direct injector was implemented numerically in the combustion chamber to investigate the mixture formation. Also, the effects of direct injection on the tumble number were studied. Moreover, the effects of the spray on wall-wetting were studied.

2- Governing Equations

The governing equations for mass conservation and momentum transport are as follows [8]:

$$\frac{\partial \rho}{\partial t} + \frac{\partial \rho u_i}{\partial x_i} = S \tag{1}$$

$$\frac{\partial \rho u_i}{\partial t} + \frac{\partial \rho u_i u_j}{\partial x_j} = -\frac{\partial P}{\partial x_i} + \frac{\partial \sigma_{ij}}{\partial x_j} + S_i \tag{2}$$

where, ρ $\left(\frac{\mathrm{kg}}{\mathrm{m}^3}\right)$ is the density, t(s) is time, u $\left(\frac{\mathrm{m}}{\mathrm{s}}\right)$ is velocity, S $\left(\frac{\mathrm{kg.m}}{\mathrm{s}}\right)$ is the term of source, and σ_{ij} $\left(\frac{\mathrm{N}}{\mathrm{m}^2}\right)$ is the viscous stress tensor; calculated as follows [10]:

$$\sigma_{ij} = \mu\left(\frac{\partial u_i}{\partial x_j} + \frac{\partial u_j}{\partial x_i}\right) + \left(\mu' - \frac{2}{3}\mu\right)\left(\frac{\partial u_k}{\partial x_k}\delta_{ij}\right) \tag{3}$$

where, in the above equation μ $\left(\frac{\mathrm{m}^2}{\mathrm{s}}\right)$ is the viscosity, μ′ is the dilatational viscosity (set to zero), δ_{ij} is the delta Kronecker.

2-1-Heat Transfer

The energy transport equation used for the simulations is as follows [10]:

$$\frac{\partial \rho e}{\partial t} + \frac{\partial u_j \rho e}{\partial x_j} = -P\frac{\partial u_j}{\partial x_j} + \sigma_{ij}\frac{\partial u_i}{\partial x_j} + \frac{\partial}{\partial x_j}\left(K\frac{\partial T}{\partial x_j}\right) + \frac{\partial}{\partial x_j}\left(\rho D\sum_m h_m \frac{\partial Y_m}{\partial x_j}\right) + S \tag{4}$$

where, ρ $\left(\frac{\mathrm{kg}}{\mathrm{m}^3}\right)$ is density, Y_m is the mass fraction of each species m, P(Pa) is the pressure, D $\left(\frac{\mathrm{m}^2}{\mathrm{s}}\right)$ is the mass diffusion coefficient, e (kJ/kg) is the specific internal energy, S is the source term, σ_{ij} is the viscous stress tensor, T(K) is the temperature, and h_m $\left(\frac{\mathrm{kJ}}{\mathrm{kg}}\right)$ is the species enthalpy.

2-2-Spray Modeling

The disintegration of spray into millions of droplets and their evaporation is produced the mixture in the combustion chamber. The local and global air-to-fuel ratio significantly are affected the combustion, fuel economy, emissions, and engine performance. In recent years, many scholars carried out experimental and numerical investigations on spray modeling, mixture formation, breakup models, and so on [9].

2-3-Primary and Secondary Breakup Models

The primary breakup model aims to simulate the fluid behavior at the nozzle exit. It considers the Kelvin-Helmholtz instabilities, which means the development of the perturbations on the liquid surface during injection in a gaseous environment. One famous model to predict the primary breakup is the wave-breakup or Kelvin-Helmholtz (KH) model, developed by Reitz [8]. The overall breakup consists of the primary and secondary breakups. Liu et al. proposed [8] a combination model for both primary and secondary breakups called the hybrid Kelvin-Helmholtz (KH) and Rayleigh-Taylor (RT) model. The RT breakup model is more dominant for the near nozzle zones, while the KH model prevails farther away. The hybrid KH-RT model showed promising results for both diesel and gasoline combustion engines [8, 9].

2-4-Collision Model

The No Time Counter model was used to model the spray collision, which is as accurate as the O'Rourke model, but much faster [9]. The base grid mesh size was considered as 2 mm, and by using Adaptive Mesh Refinement and fixed embedding with a scale of 3, the mesh size during spray injection, collision, and evaporation was refined up to 0.25 mm in some zones. The mesh size of 0.25 mm for spray parcel zones was accurate enough according to the results of Ref. [9]. The parcel number of 480000 showed accurate results and good agreement with experimental data. Higher parcel numbers (higher than 2,400,000) showed poor results due to the overestimation of liquid penetration and general underestimation of the drag forces in injector engines [9].

2-5-Wall Impingement Model

The injected fuel jet in the combustion chamber impacts the piston surface and affects the combustion characteristics and emission formation. The fuel jet and wall interactions can be divided into four regimes based on the Webber Number and wall temperature [9], including:

- Stick
- Rebound
- Spread
- Splash

The O'Rourke wall impingement model was used to simulate all the regimes and the interactions between the spray droplets and the wall surface.

2-6-Turbulent Regime Modeling

The Generalized Re-Normalization Group (GRNG) k-ε model was applied to predict the turbulent regime. This model is appropriate for the reacting and non-reacting compressible flows, especially in the case of Internal Combustion Engines (ICEs). The (GRNG) k-ε model governing equation is as follows [9]:

$$\rho\frac{D\varepsilon}{Dt}=\frac{\varepsilon}{k}C_1P+C_1^{'}\rho v_t\frac{\varepsilon}{k}(\nabla.u)^2-C_{2n}\rho\frac{\varepsilon^2}{k}-\rho R+C_3\rho\varepsilon(\nabla.u)+diffusion \quad (5)$$

where, the model parameters are calculated as follows:

$$C_1^{'} = a\left(1 - \frac{2}{3}C_1\right)$$
$$C_{2n} = b_0 + b_1 n + b_2 n^2$$
$$C_3 = -\frac{n+1}{n} + \frac{2}{3}C_1 + \sqrt{\frac{2(1+a)}{3}}\, C_\mu C_\eta \eta (-1)^\delta \quad (6)$$
$$C_\eta = \frac{\eta\left(1 - \frac{\eta}{\eta_0}\right)}{1 + \beta\eta^3}$$

In the intake stroke, a tumble flow typically occurs and continues into the compression stroke until the piston is close to Top Dead Center (TDC). The level of tumble is measured using tumble ratios, namely TRx and TRy. These ratios are defined based on the angular velocities of a solid body rotating flow in the y-z plane (ω_x) and x-z plane (ω_y), respectively.

3- Computational Approach and Methodology

A CFD model was developed to port design to optimize tumble number in the combustion chamber of the EC5+ (Turbo-Charged) engine for the condition of fully open throttle and the engine speed of 6000 rpm. The CFD model predicts an open-cycle engine exchange from 0 °ATDC to 720 °ATDC. For modeling the turbulence regime of the fluid flow, the Generalized Re-Normalization Group (GRNG) k-ε model was applied.

4- Simulation Setup

Figure 1 displays the geometry of the GDI engine combustion chamber. The GDI engine specifications are given in Table 1. The computational mesh is generated at each runtime during the CFD simulation. The geometry of a mesh is composed of any arbitrary number of logical blocks that are patched together in a completely seamless fashion. The movement of the piston/flow domain is resolved using the boundary motion. As the piston moves during the solution process, the internal mesh structure deformed automatically to optimize the mesh. The distortion of each cell occurs; when the generated cell distortion reaches a certain level, the solution is re-zoned onto a new mesh. Figure 1 illustrates the fluid domain of the simulation, such as the inlet ports, exhaust ports, and combustion chamber geometries in the CONVERGE CFD tool. The cell number ranged from 110468 at TDC to 741523 at BDC for the computational grids. Mesh independency was investigated by variation of cell number from 50231 to 143784 on in-cylinder maximum pressure.

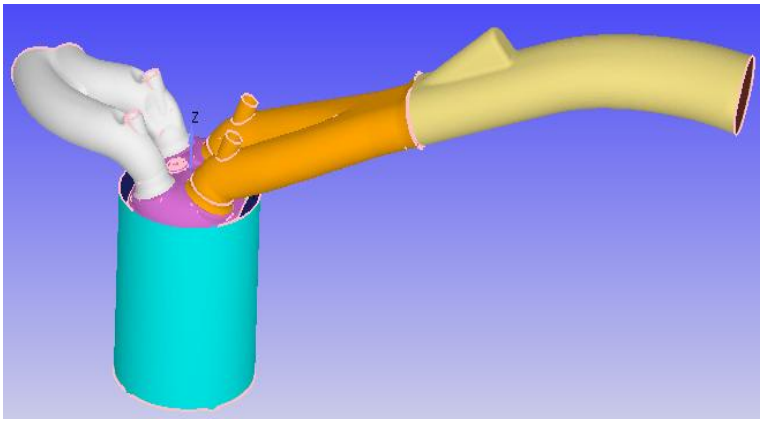

Figure 1 The geometry of the engine combustion chamber

Table 1 The engine specifications

Bore	77 mm	Engine Speed	5500 rpm
Stroke	93 mm	Fuel	Gasoline
Compression ratio	9.7	Connecting rod length	134.5 mm
Displacement volume	1299.2 cc	Start of injection	379 BTDC
Inlet valve diameter	30 mm	Injection duration	170 CAD
Exhaust valve diameter	26 mm	Injection pressure	350 bar
Intake valve timings	IVO = 366° ATDC IVC = 598° ATDC	Exhaust valve timings	EVO = 126° ATDC EVC = 385° ATDC

5- Initial and Boundary Conditions

Computation starts at 270 deg before TDC overlap. Initial data for the start of the simulation were selected from GT POWER results. Figure 2 shows the transient boundary condition of mass flow rate and temperature versus crank angle imposed on the air runner. Figure 3 shows the transient boundary condition of pressure and temperature versus the crank angle imposed on the exhaust port.

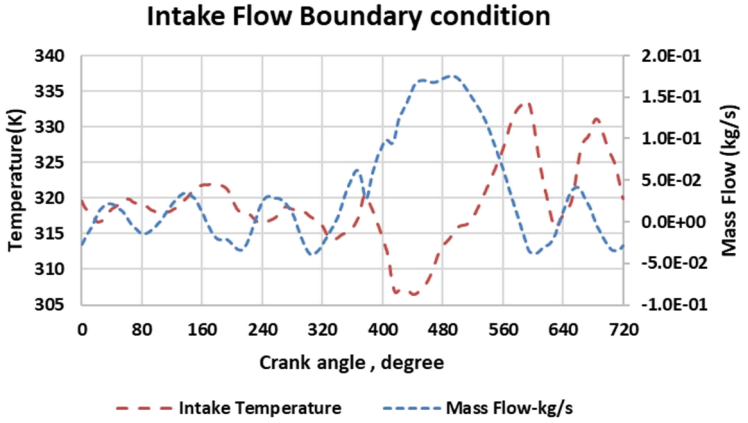

Figure 2 Transient boundary condition at air runner versus crank angle: mass flow and temperature

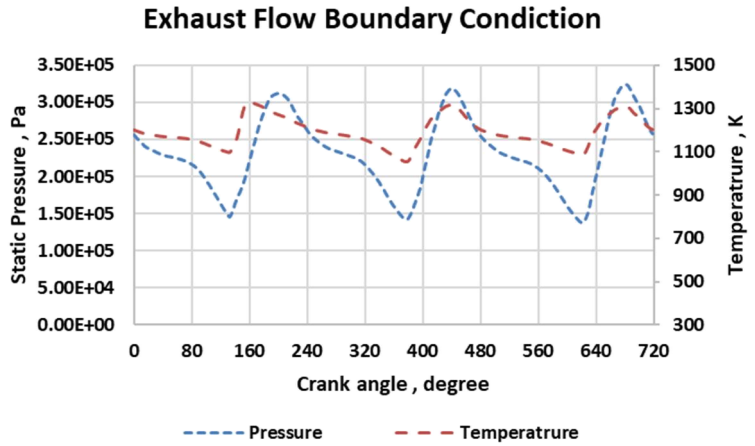

Figure 3 Transient boundary condition at exhaust port versus crank angle: pressure and temperature

The temperature was taken as 452 K for the liner, 403 K for the cylinder head and piston, 542 K for the intake valve, and 673 K for the exhaust valve. All boundary conditions were validated with the experimental data.

6- Validation study

Figure 4 illustrates the experimental and CFD pressure versus crank angle degree (time). Comparison between CFD and experiment shows good agreement. The maximum error is 5 percent.

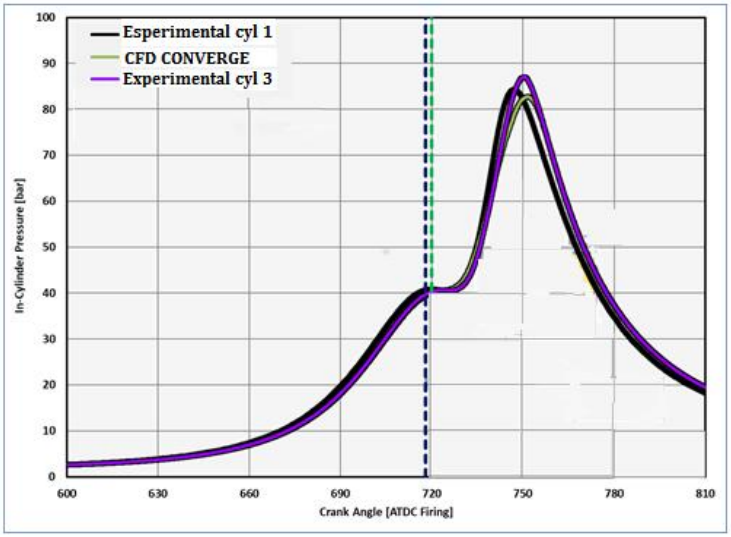

Figure 4 Experimental and CFD in-cylinder pressure versus crank angle degree

7- Results and Discussion

Figure 5 depicts the peaks of the tumble number during the intake and compression strokes. When the intake valve lift is maximum, the tumble number is at its maximum level of about -0.75. Another peak occurs at about 90 to 60 degrees before TDC. This figure also specifies the best timings with maximum tumble number levels with this specific intake port and combustion chamber geometry. These crank angle degrees (CADs) are the best timing for sequential direct injections for the same GDI engine.

Figure 6 depicts the spray evolution, lambda distribution, and droplet temperature from the 40 Crank Angle Degrees (CAD) after the Start of Injection (SOI) until the End Of Injection (EOI). At 40 CAD after SOI, the local excess air-to-fuel ratio (Lambda or λ) varies from 0.5 to 1.5. The zones of $\lambda = 1.5$, where excess air exists, are the regions that are far from the injector.

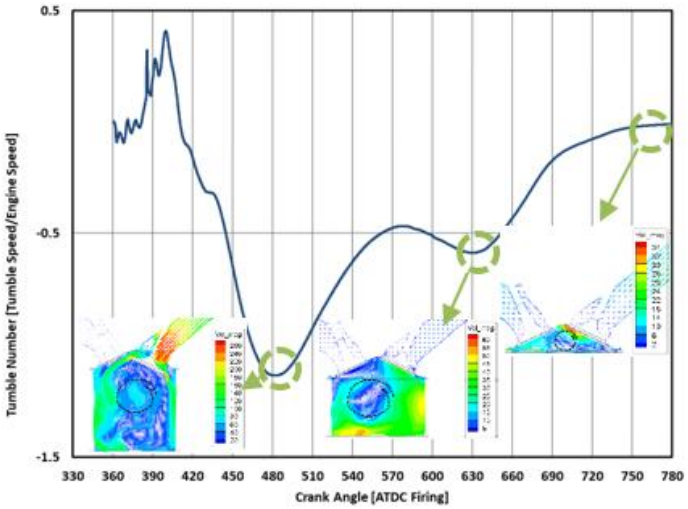

Figure 5 Tumble number versus crank angle

Lambda distribution Droplet temperature

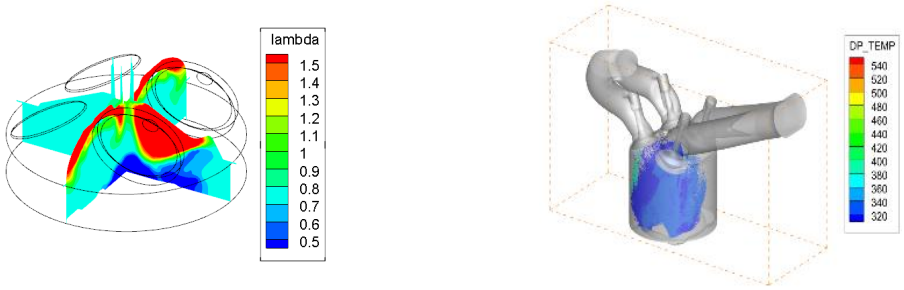

40 Deg after TDC – 30 Deg after Injection Initiation

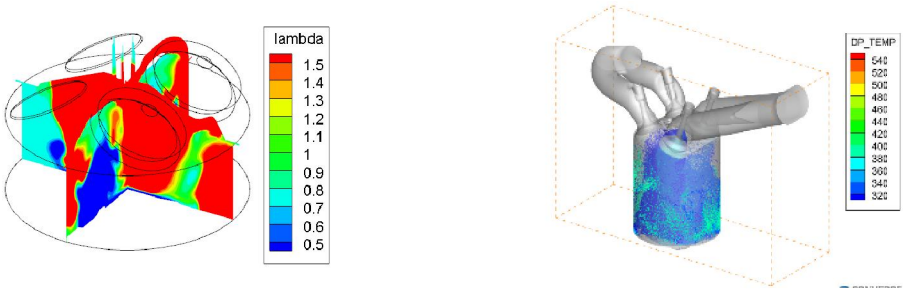

60 Deg after TDC 70 Deg after Injection Initiation

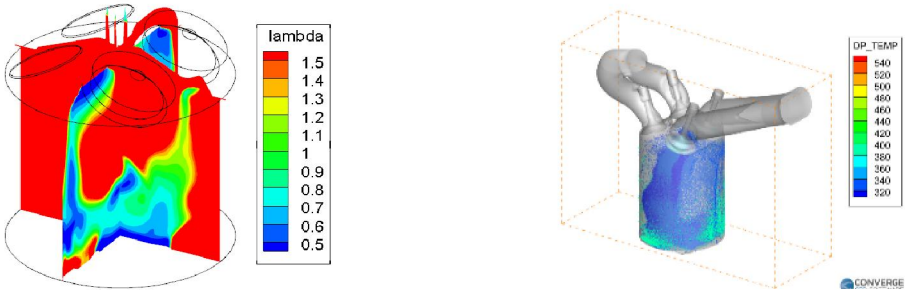

120 Deg after TDC – 100 Deg after Injection

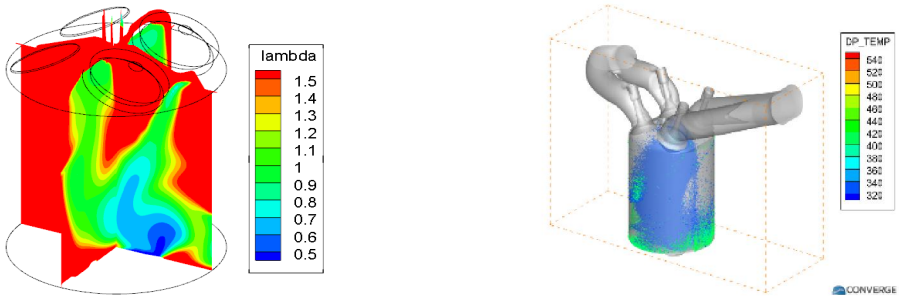

170 Deg after TDC – 150 deg after Injection

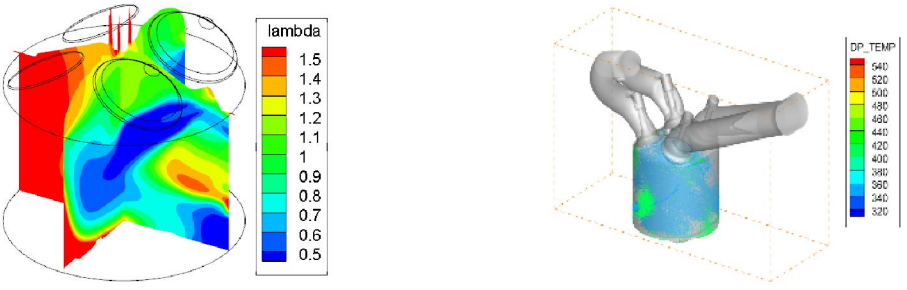

270 Deg after TDC – 250 deg after Injection End of the injection

Figure 6 Mixture formation investigation Droplets distribution and lambda during injection

Conversely, in the regions near the injector (or in the spray cone), λ is about 0.5, much richer. In addition, the spray droplet temperatures are about 295 K near the nozzle, and it increases up to about 370 K to be vapored and make a homogenous mixture. At the End of Injection (EOI), the excess air to fuel mixture (λ) becomes more homogenous but not fully homogenous. The average spray droplet temperature reached about 360 K, showing that most parcels have not been vaporized at this CAD. The cooling-charge effect of the spray is evident at this CAD, which is an excellent advantage of the GDI engines. On the contrary, some parcels with temperatures of about 380K or more have not been vaporized and stick to the cylinder wall and piston surfaces. They are the primary sources of Particulate Matter (PM), which is one of the main drawbacks of the GDI engines. Temperature distribution in the cross-section through the mid-plane of the spark plug is shown in Figure 7 Due to high tumble flow in the cylinder of GDI, the flame front moves to the exhaust side of the combustion chamber. The maximum temperature is 2500 K.

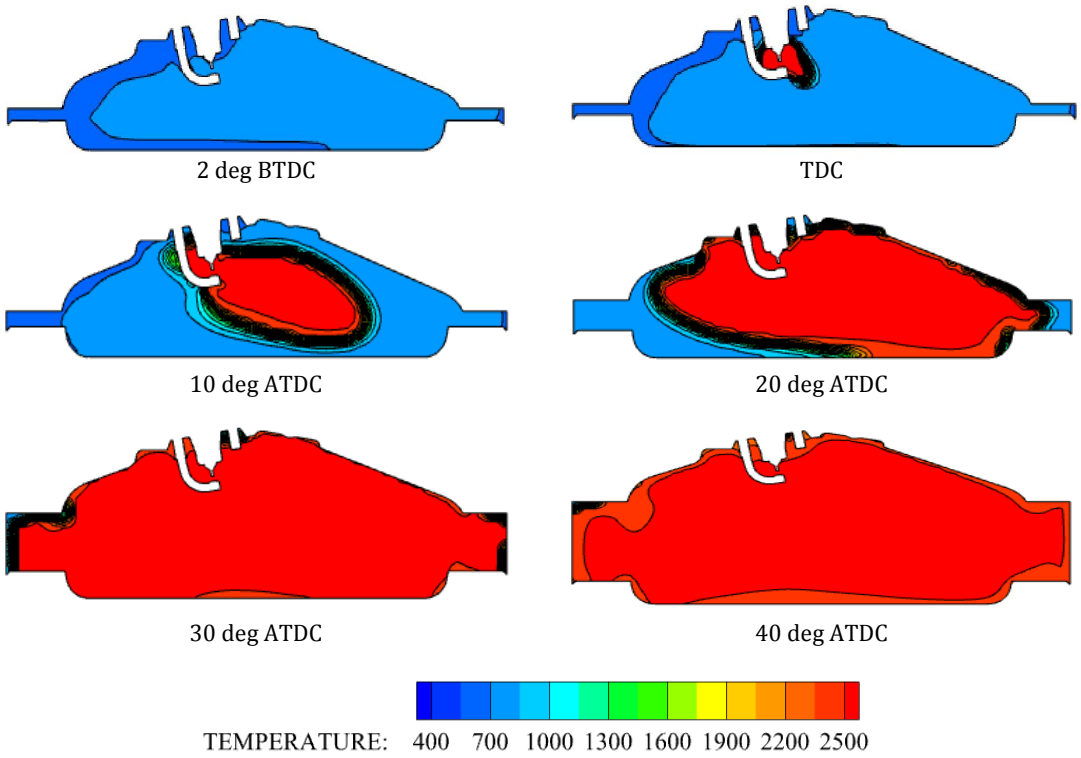

Figure 7 Temperature distribution in the cross-section through the midplane of spark plug

Figure 8 describes the curves of the evaporated fuel mass over time. The mass of evaporated fuel during the sparking represented no more than 40% of the injected fuel mass for low engine temperatures. This evaporation ratio increased up to 60% for high engine temperatures. It can be expected for the low engine temperature that a part of the fuel would probably never evaporate even during the combustion, mainly due to wall-wetting. This would explain why the injection of a fuel mass more than the stoichiometric one is required, especially under these conditions.

Figures 9-11 depict the wall film or the parcels and wall-wetting effects from the SOI until the end of injection. The fuel mass on the piston surface during the injection is higher than on the liner surface. Thus, the piston surface affects the mixture preparation and emissions formation (especially PM). In addition, the piston surface can be optimized in the next studies to properly guide spray droplets near the spark plug and make appropriate mixture stratification to have better combustion from the standpoint of emission and fuel economy.

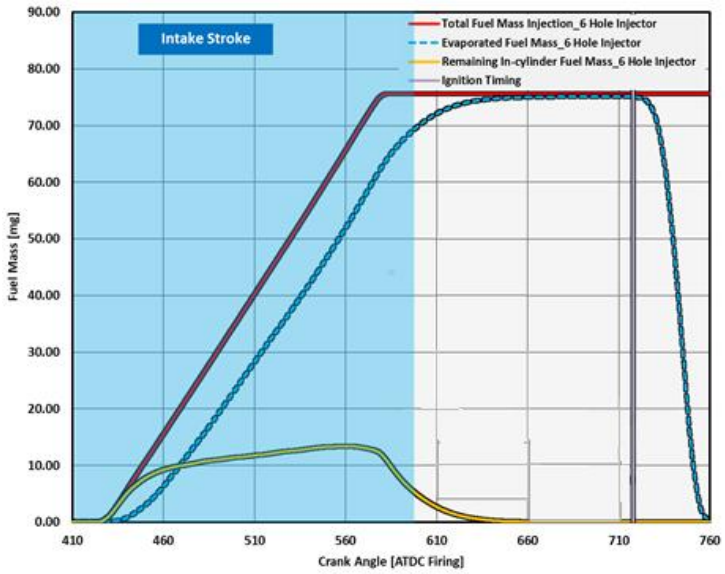

Figure 8 Liquid and evaporated fuel versus crank angle

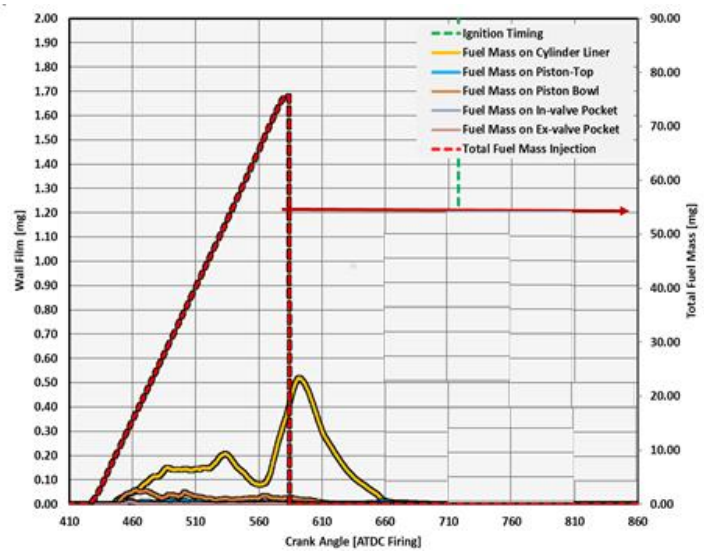

Figure 9 Wall film mass on the piston and liner

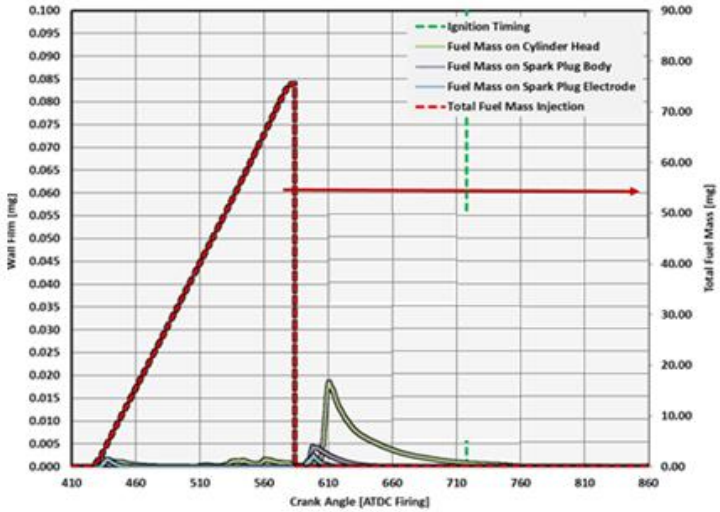

Figure 10 Wall film mass on the cylinder head

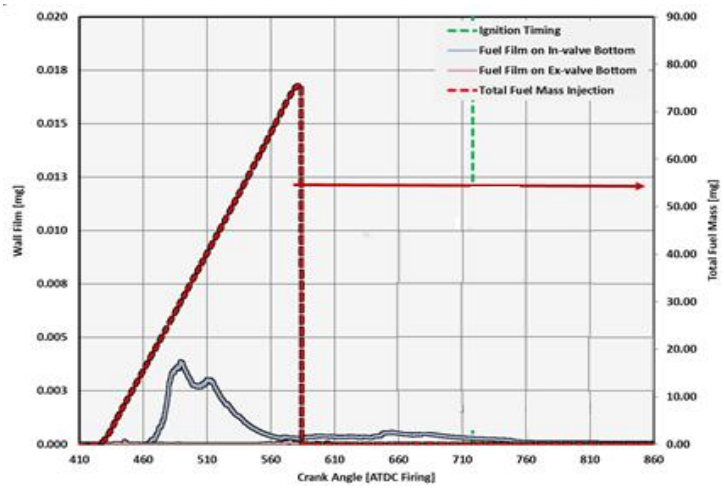

Figure 11 Wall film mass on the intake and exhaust valves

Figure 12 displays air-fuel distribution at ignition time. Due to this graph, 50% of the equivalence ratio is between 1.1 to 1.2, so the flame is stable in these conditions.

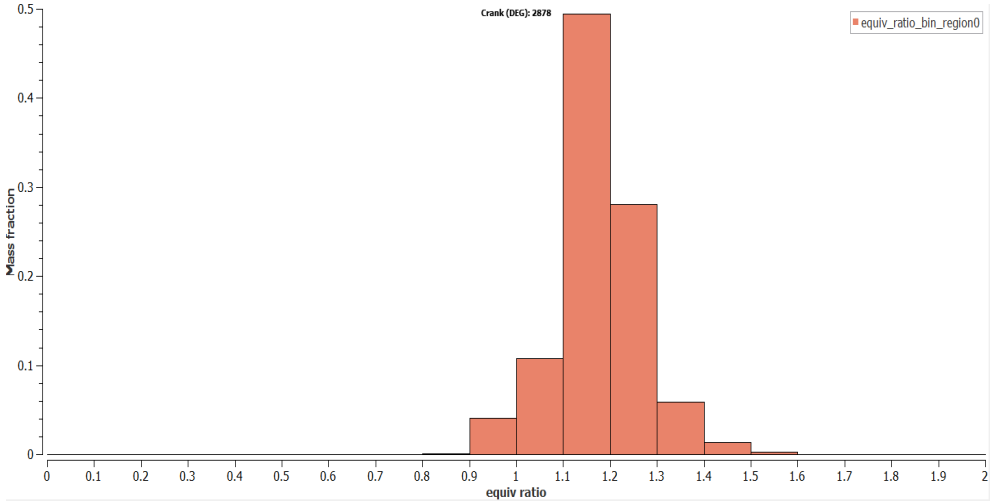

Figure 12 Air-fuel distribution at ignition time

8- Conclusions

A 3D-CFD model was developed for the 3-cylinder GDI engine to numerically investigate the spray and combustion evolution in the combustion chamber while using the gasoline direct injection (GDI) strategy at the speed of 5500 rpm and wide-open throttle conditions. The main results are as follows:

1) CFD results showed the lambda distribution at the ignition timing. Near the spray zones, lambda is about 0.7, but in some regions far from the injector, lambda increased up to 1.5, which are the zones contributing to thermal NO_X formation.

2) The CFD results showed the mixture homogeneity needs to be improved at the operating conditions of 5500 rpm and wide-open throttle.

3) The piston surface had higher liquid wall films than the liner, which shows that optimizing the piston profile is necessary to minimize the wall-wetting effect.

References

[1] Amsden AA. KIVA-3V, release 2: improvements to KIVA-3V. Los Alamos National Lab.(LANL), Los Alamos, NM (United States); 1999 May 1.

[2] Group CA. STAR-CD Version 3.26 User's Guide; 2008.

[3] Bianchi GM, Richards K, Reitz RD. Effects of initial conditions in multidimensional combustion simulations of HSDI diesel engines. SAE Technical Paper; 1999 Mar1. doi: 10.4271/1999-01-1180:10
[4] Wegner B, Maltsev A, Schneider C, Sadiki A, Dreizler A, Janicka J. Assessment of unsteady RANS in predicting swirl flow instability based on LES and experiments. International Journal of Heat and Fluid Flow. 2004 Jun 1;25(3):528-36. doi: 10.1016/j.ijheatfluidflow.2004.02.01
[5] Chow WK, Li J. Numerical simulations on thermal plumes with k–ε types of turbulence models. Building and Environment. 2007 Aug 1;42(8):2819-28. doi: 10.1016/j.buildenv.2005.12.006
[6] Gilmore J, Jermy M. CFD study of wake decay and separation regions in jet engine test facilities. In Proceedings of the 16th Australasian Fluid Mechanics Conference; 2007; Crown Plaza, Gold Coast, Australia.
[7] Bardow A, Bischof CH, Bücker HM, Dietze G, Kneer R, Leefken A, Marquardt W, Renz U, Slusanschi E. Sensitivity-based analysis of the κ-ε model for the turbulent flow between two plates. Chemical Engineering Science. 2008 Oct 1;63(19):4763-75. doi: 10.1016/j.ces.2007.12.029
[8] FLUENT manuals. 2015.
[9] Sadakane S, Sugiyama M, Kishi H, Abe S, Harada J, Sonoda Y. Development of a new V-6 high performance stoichiometric gasoline direct injection engine. SAE Technical Paper; 2005 Apr 11. doi: 10.4271/2005-01-1152
[10] Zhang Z, Li A, Zheng Z. Numerical simulation research on the influence of the parameters of water injection on the GDI engine. International Journal of Engine Research. 2023 Jun;24(6):2568-91. doi: 10.3390/pr10101909
[11] Zhang Z, Dai X, Zheng Z. Numerical Simulation Study on the Effect of Port Water Injector Position on the Gasoline Direct Injection Engine. Processes. 2022 Sep 21;10(10):1909.
[12] Li X, Li D, Dimitriou P, Ajmal T, Aitouche A, Mobasheri R, Rybdylova O, Pei Y, Peng Z. Comparative investigation on macroscopic and microscopic characteristics of impingement spray of gasoline and ethanol from a GDI injector under injection pressure up to 50 MPa. Energy Reports. 2023 Dec 1;9:1910-8. doi: 10.1016/j.egyr.2023.01.024
[13] Oh H, Hwang J, White L, Pickett LM, Han D. Spray collapse characteristics of practical GDI spray for lateral-mounted GDI engines. International Journal of Heat and Mass Transfer. 2022 Jul 1;190:122743. doi: 10.1016/j.ijheatmasstransfer.2022.122743
[14] Lu L, Pei Y, Qin J, Peng Z, Wang Y, Zhong K. Experimental study on spatial distribution characteristics of cylinder-wall oil films under fuel spray impinging condition of GDI engine. Energy. 2022 Sep 1;254:124381. doi: 10.1016/j.energy.2022.124381
[15] Qiao J, Liu J, Zhang Q, Liang J, Wang R, Zhao Y, Shen D. Experimental investigation on the effects of Miller cycle coupled with asynchronous intake valves on the performance of a high compression ratio GDI engine. Fuel. 2023 Jan 15;332:126088. doi: 10.1016/j.fuel.2022.126088
[16] Muddapur A, Sahu S, Jose JV, Sundararajan T. Spray–wall impingement in a multi-hole GDI injector for split injection at elevated wall temperature and ambient conditions. Thermal Science and Engineering Progress. 2022 Aug 1;33:101367. doi: 10.1016/j.tsep.2022.101367
[17] Berni F, Sparacino S, Riccardi M, Cavicchi A, Postrioti L, Borghi M, Fontanesi S. A zonal secondary break-up model for 3D-CFD simulations of GDI sprays. Fuel. 2022 Feb 1;309:122064. doi: 10.1016/j.fuel.2021.122064

نشریه علمی تحقیقات موتور
زمستان ۱۴۰۲، جلد ۷۰، شماره ٤، صفحه ۱-۱۳
تارنمای نشریه: www.engineresearch.ir

مقاله پژوهشی

شبیه‌سازی دینامیک سیالات محاسباتی لایه سوخت روی دیواره در هنگام پاشش سوخت و احتراق در موتوری سه‌استوانه تزریق مستقیم پرخوران

آرش محمدی[۱*]، نیما عجمی[۲]، امیر حسین پریور[۲]، پیمان شرقی[۲]

[۱] دانشکده مهندسی مکانیک، دانشگاه تربیت دبیر شهید رجایی، تهران، ایران
[۲] مرکز تحقیقات موتور ایران‌خودرو (ایپکو)، تهران، ایران

اطلاعات مقاله

کلیدواژه‌ها:
موتور بنزینی پاشش مستقیم
افشانه سوخت
آماده‌سازی مخلوط
شبیه‌سازی افشانه

چکیده

در این پژوهش، الگوی سه بعدی دینامیک سیالات محاسباتی برای بررسی رفتار افشانه سوخت و احتراق در موتوری سه‌استوانه با استفاده از افشانه شش سوراخ ایجاد شد. برای اعتبارسنجی الگو، فشار داده درون استوانه در شرکت تحقیقات موتور ایران خودرو (ایپکو) تحت شرایط دریچه گاز کاملاً باز و ۵۵۰۰ دور در دقیقه انجام شد. داده‌های به‌دست‌آمده در الگوی دینامیک سیالات محاسباتی برای شبیه‌سازی تزریق افشانه و فرآیند احتراق در داخل استوانه در طول تزریق سوخت گنجانده شد. دمای قطره و توزیع لامبدا طی ۳۰ تا ۲۷۹ درجه پس از تزریق نمایش داده شدند. توزیع دما در طول ۲ تا ۴۰ درجه بعد از نقطه مکث بالا در مقاله نشان داده شده است. در نهایت سوخت تبخیر شده و لایه سوخت دیواره بستار، آستر، سمبه و دریچه‌های ورودی و خروجی بررسی شده است.

* نویسنده مسئول
پست الکترونیکی: amohammadi@sru.ac.ir (آرش محمدی)

دریافت ۸ اردیبهشت ۱۴۰۳؛ پذیرش ۳۰ اردیبهشت ۱۴۰۳
شاپای الکترونیکی: ۴۱۲۱-۲۳۴۵ / شاپای چاپی: ۵۲۱۴-۱۷۳۵

Cite this article: Mohammadi A, Ajami N, Parivar AH, Sharghi P. CFD simulation of wall film during fuel injection and combustion in a three-cylinder turbocharged gasoline direct injection engine. The Journal of Engine Research. 2024 Feb 20;70(4):1-13. doi: 10.22034/ER.2024.2025014.1034